JCEC
THE JOURNAL OF ENGINEERING AND EXACT SCIENCES

OPEN ACCESS

The Journal of Engineering and Exact Sciences – jCEC, Vol. 08 N. 07 (2022)
journal homepage: https://periodicos.ufv.br/jcec
eISSN: 2527-1075
ISSN: 2446-9416

Synthesis, Characterisation, Theoretical NMR Calculations and Crystal Structure of the 3-methyl-1*H*-1,2,4λ^4-triazole-5-amine acetate

Síntese, Caracterização, Cálculos Teóricos de RMN e Estrutura Cristalina do 3-metil-1*H*-1,2,4λ^4-triazol-5-amina acetato

Article Info:
Article history: Received 2022-03-06/ Accepted 2022-09-21 / Available online 2022-09-21
doi: 10.18540/jcecvl8iss7pp14608-01i

Patricia Saraiva Vilas Boas de Almeida
ORCID: https://orcid.org/0000-0001-7205-2115
Departamento de Química, Universidade Federal de Viçosa, Brazil
E-mail: pvilasboas@yahoo.com.br
José Roberto da Silveira Maia
ORCID: https://orcid.org/0000-0001-5715-8763
Departamento de Química, Universidade Federal de Viçosa, Brazil
E-mail: jrsmaia@ufv.br
Márcia Cristina de Souza
ORCID: https://orcid.org/0000-0001-8333-3617
Departamento de Química, Universidade Federal de Juiz de Fora, Brazil
E-mail: marciaphn@gmail.com
Alison Geraldo Pacheco
ORCID: https://orcid.org/0000-0003-1338-0340
Instituto Federal de Educação, IFSULDEMINAS, Brazil
E-mail: alison.pacheco@ifsuldeminas.edu.br

Resumo
A reação de condensação entre bicarbonato de aminoguanidina com ácidos carboxílicos levou à formação de 3-metil-1S-1,2,4-triazol-5-amine (mta), 3-metil-1H-1,2,4□4-triazole-5-amine acetato (Hmta) e 3-fenil-1H-1,2,4-triazole-5-amine (pta). O composto N-(3-metil-1S-1,2,4-triazole-5-yl)propan-2-imine (mpta) foi obtido reagindo a mta com acetona, após uma tentativa de purificar mta neste solvente. O excesso de ácido acético obteve o Hmta durante a preparação do mta. Esses compostos foram caracterizados por espectroscopia infravermelha e multinuclear de NMR (1H e 13C), microanálise e ponto de fusão. Para investigar a formação de possíveis conformações tautoméricas de mta, pta e mpta em solução, utilizou-se uma abordagem teórica para calcular as mudanças químicas do carbono 13, com base nos valores do tensor de blindagem magnética (NMR) pelos métodos MPn e DFT. O ensaio biológico dos triazoles mta, pta e mpta contra Staphylococcus aureus, Bacillus subtilis, Escherichia coli e *Salmonella typhimurium* não mostrou atividade na maior concentração utilizada no experimento.
Palavras-chave: Compostos 1,2,4-Triazois. Testes biológicos. Estrutura cristalina. Espectroscopia.

Abstract
The condensation reaction between aminoguanidine bicarbonate with carboxylic acids led to the formation of 3-methyl-1*H*-1,2,4-triazole-5-amine (*mta*), 3-methyl-1*H*-1,2,4λ^4-triazole-5-amine acetate (*Hmta*) and 3-phenyl-1*H*-1,2,4-triazole-5-amine (*pta*). The compound N-(3-methyl-1*H*-1,2,4-triazole-5-yl)propan-2-imine (*mpta*) was obtained by reacting the *mta* with acetone, upon an attempt of purifying *mta* in this solvent. The excess of acetic acid obtained the *Hmta* during the preparation of *mta*. These compounds were characterised by infrared and multinuclear NMR (^{1}H

and ^{13}C) spectroscopy, microanalysis, and melting point. To investigate the formation of possible tautomeric conformations of *mta*, *pta* and *mpta* in solution, a theoretical approach was used to calculate the chemical shifts of carbon 13, based on the values of magnetic shielding tensor (NMR) by MPn and DFT methods. The biological assay of the triazoles *mta, pta* and *mpta* against *Staphylococcus aureus*, *Bacillus subtilis*, *Escherichia coli* and *Salmonella typhimurium* showed no activity at the highest concentration used in the experiment.
Keywords: 1,2,4-Triazole compounds. Biological assay. Crystal structure. Spectroscopy.

1. Introduction

Triazole compounds are acknowledged as antifungal, antiviral, antibacterial, antidepressant and anticonvulsant drugs (Deng, Song, Zheng, & Quan, 2014; Naito et al., 1996; Papakonstantinou-Garoufalias, Pouli, Marakos, & Chytyroglou-Ladas, 2002). The treatment of human diseases involves several triazoles as *Fluconazole*, *Itraconazole* and *Ravuconazole* (Johnson, Szekely, & Warnock, 1999; Roberts, Schock, Marino, & Andriole, 2000). The *Itraconazole*, for instance, prevent the enzyme sterol 14-alpha demethylase to interact with the iron(II) ion on the haem of the enzyme becoming the key-step for the biosynthesis of ergosterol (Groll, Piscitelli, & Walsh, 1998). The *Ribavirin* is an antiviral agent of large spectrum for the treatment of pathological illnesses of the lower respiratory tract in humans (Graci & Cameron, 2006). The 1,2,4-triazole compounds are also known to inhibit the mitochondrial and chloroplast function. This property allows these compounds to be commercialised in the market like herbicides, defoliant on cotton farming and in the control of plant growth (Han et al., 2011).

These compounds are capable of forming hydrogen bond which might favour specific biochemical interactions within a living organism (Vatmurge et al., 2008). Triazole compounds containing large carbon chain or aromatic groups bonded to the ring of 1,2,4-triazole showed positive response to the antimicrobial assay (El Akri, Bougrin, Balzarini, Faraj, & Benhida, 2007; Karthikeyan, Holla, & Kumari, 2008).

Considering the activity of the 1,2,4-triazole derivatives, a few compounds with small group substituent bonded to the ring were synthesised, characterised and assayed in this work against *Staphylococcus aureus*, *Bacillus subtilis*, *Escherichia coli* and *Salmonella typhimurium* to evaluate their potential as antibiotics.

The labile nature of the hydrogen atom probably leads to tautomeric species in solution. Stable tautomers can be identified by NMR spectroscopy if the labile hydrogen bind to different atoms, such as nitrogen and sulfur (Wu et al., 2007). Beyond the characterization by infrared and NMR techniques of the triazole compounds in this work, a theoretical approach using the magnetic shielding tensor was carried out to investigate a possible tautomerism in solution, by comparing the calculated and experimental NMR data (Phalgune, Vanka, & Rajamohanan, 2013).

2. Results and discussion

Several condensation reactions are reported in the literature for the preparation of triazole compounds. The usual reagents in the synthetic route of triazoles are acylimidazones (Pellizzari reaction), diacylamines or hydrazine (Einhorn-Brunner reaction), and 1,2-diacylhydrazine (Sudheendran, Schmidt, Frey, Conrad, & Beifuss, 2014). Although these reagents are well known, aminoguanidine bicarbonate was chosen as starting material because is inexpensive and simple to manipulate in the process of purification before attempting the experiment. This compound was also used as reactant in the synthesis of 5-amino-1*H*-1,2,4-triazole-3-acetic acid and 3-amine-5-methyl-1*H*-1,2,4-triazole or 3-methyl-1*H*-1,2,4-triazole-5-amine (*mta*) through the condensation reaction with carboxylic acids (Boechat, Pinheiro, Santos-Filho, & Silva, 2011). The molecular structures of the 1,2,4-triazole compounds in this work are shown by Figure 1.

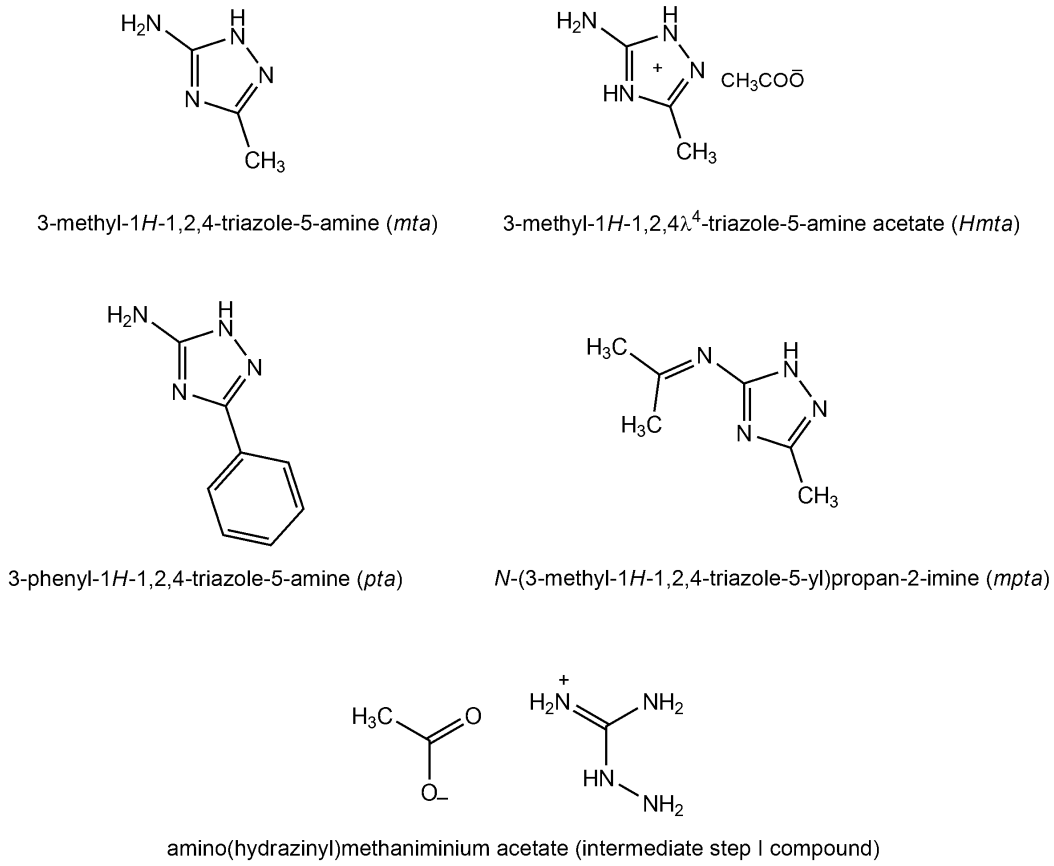

Figure 1 - Molecular structure of the 1,2,4-triazole compounds and a possible intermediate compound (step I).

The triazole compound *mta* was synthesised by the equimolar reaction between the aminoguanidine bicarbonate and the acetic acid as well as the *pta* with the benzoic acid. However, a subsequent acid/base reaction took place by the use of an excess of acetic acid (60%), forming the *Hmta*, to which the crystal structure has been analysed. A few crystals of *Hmta* also separated after cooling the filtrate from the equimolar synthesis of the *mta*. The attempt of purifying *mta* in acetone produced the *mpta* as the main product. This product allow us to speculate that a small amount of unreactive acetic acid catalysed the reaction between *mta* and acetone. These triazole compounds are soluble in dimethyl sulfoxide, methanol, and chloroform. The reaction route to produce these 1,2,4-triazole derivatives is shown by Figure 2. ^{13}C NMR characterized the intermediate step (I) compound, separated by filtration at room temperature.

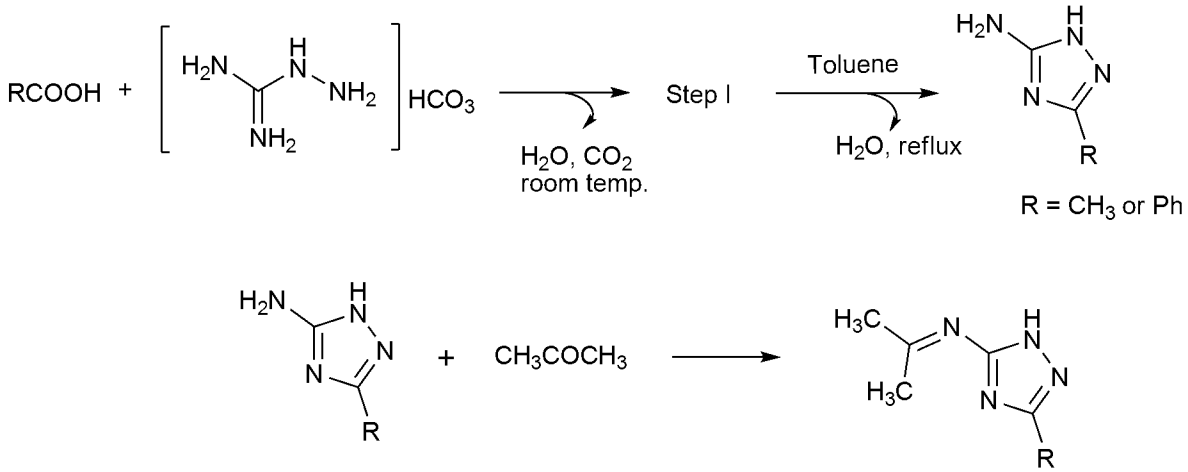

Figure 2 - Synthetic route to the preparation of the 1,2,4-triazole compounds.

2.1. Infrared Spectroscopy

The infrared spectrum of aminoguanidine bicarbonate showed three strong bands in the region of 3245 cm^{-1} correlated to the stretching vibrational modes ν(N-H) and the bicarbonate ion shown a strong infrared absorption at 1355 cm^{-1}. Absorptions in the range of 1720 to 1600 cm^{-1} were assigned to the carbonyl group of the carboxylic acids (Silverstain, Bassler, & Morril, 1991; Vieira, Maia, Ardisson, & de Lima, 2008). A typical infrared band in the range of 3300 to 2500 cm^{-1}, characteristic of intramolecular hydrogen bond between the hydroxyl group and the carbonyl group, was also shown in the spectra of these carboxylic acids (Silverstain et al., 1991).

The condensation reaction between the aminoguanidine and the carboxylic acids was confirmed by an infrared vibrational shift to high frequency of the amine group (Boechat et al., 2011; Vieira et al., 2008). Two infrared bands identified in the range of 3289 to 3317 cm^{-1} correlates to the NH_2 group of the *mta* and *pta* compounds. Furthermore, the absence of the intramolecular hydrogen bond of carboxylic acids in the spectra of these compounds reinforces the formation of the triazole derivatives.

The infrared spectroscopy has been a useful technique to characterize tautomers of the triazole compounds class. The infrared bands of the C=N group in the range of 1700 to 1600 cm^{-1} have been related to the formation of tautomeric species of 1,2,4-triazoles at equilibrium due to the N-H bond configurations on the ring (Akerblom & Sandberg, 1965; Grinshtein, Strazdin, & Grinvalde, 1970; Lopyrev, Beresneva, & Strelets, 1969). The 3-Chloro-1,2,4-triazole revealed two infrared bands at 1770 and 1750 cm^{-1} that have been assigned to tautomeric species (Grinshtein et al., 1970). The compound diamine-1,2,4-triazole also showed two bands in the range of 1600 to 1640 cm^{-1} associated to the formation of tautomeric species (Abdel-Megeed, Abdel-Rahman, Alkaramany, & El-Gendy, 2009; Lopyrev et al., 1969; Tyagi et al., 2017; Wajda-Hermanowicz et al., 2016).

The number of infrared bands relative to the C=N bond of the triazole compounds in this work are in agreement with the presence of isomeric forms in the solid state, as previously reported in the literature. The strong infrared absorption at 1633 cm^{-1}, that corresponds to ν(C=N) of the aminoguanidine bicarbonate, has split up in two new absorptions in the range of 1705 to 1575 cm^{-1} in the spectra of the triazoles *mta*, *pta* and *mpta*. The third additional infrared absorption for the *mpta* compound at 1579 cm^{-1} was assigned to the ν(C=N) of the imine group outside of the triazole ring, similar to other Schiff bases derivatives (Sokmen et al., 2015; Tyagi et al., 2017; Wajda-Hermanowicz et al., 2016).

The synthesis and characterisation of *mta* (3-methyl-1*H*-1,2,4-triazole-5-amine) is reported in the literature but the acetate salt derivative, 3-amine-5-methyl-1*H*-1,2,4λ^4-triazole (*Hmta*), is an original compound (Boechat et al., 2011). Possible tautomeric species of *mta* (A', B', C') and *pta* (A, B, C, D, E), as well as of *mpta* (F, G, H, I, J, K) are shown by Figure 3.

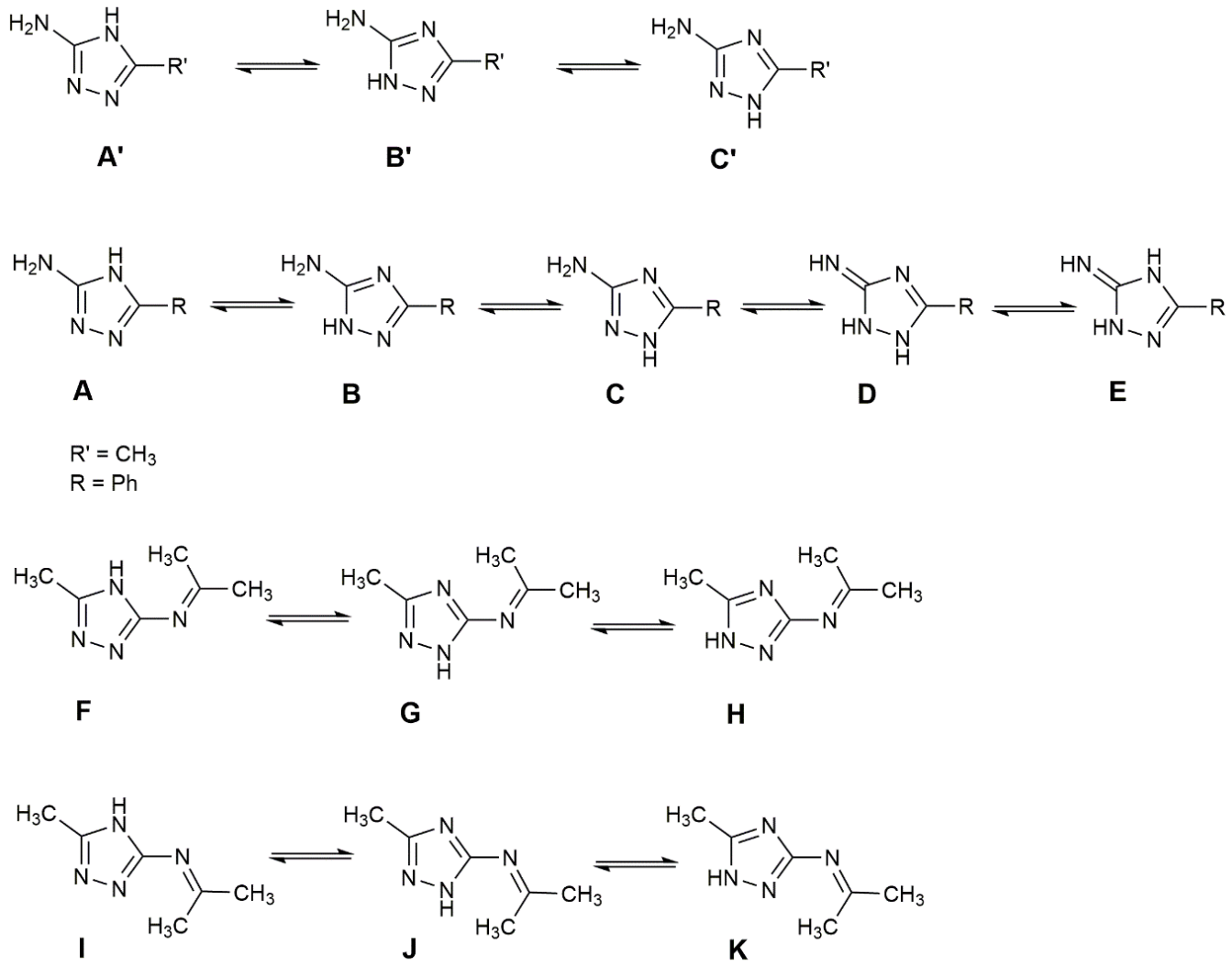

Figure 3 - Possible tautomeric species of *mta* (A′, B′, C′), *pta* (A, B, C, D, E) and *mpta* (F, G, H, I, J, K).

2.2. NMR Spectroscopy

The hydrogen NMR of *pta* in DMSO showed broad singlets correlated to the primary amine group (NH_2) at δ 8.13, and at δ 10.32, associated to the pyrrole group (NH) from the 1,2,4-triazole ring. In $CDCl_3$, the chemical shift for the amine group from *pta* was at δ 8.24 and for the pyrrole group at δ 10.45. The hydrogen atoms of the phenyl group from *pta* showed signals in the region of δ 7.31 in DMSO, CD_3OD and $CDCl_3$. The $J(^1H\text{-}^1H)$ coupling constant for these hydrogen atoms is 7.21 Hz confirming the presence of this group in the structure of the compound (Silverstain et al., 1991). A broad singlet at δ 11.06 (DMSO) in the spectrum of *mpta* correlates to the pyrrole group and the methyl groups for this compound shown chemical shifts at δ 2.17, 2.04 and 1.88 in DMSO.

The spectrum of *mta* reported in the literature, nomenclature of 3-amine-5-methyl-1*H*-1,2,4-triazole or 3-methyl-1*H*-1,2,4-triazole-5-amine has revealed two broad hydrogen signals in DMSO in the range of δ 8.7 to δ 8.0 and δ 6.3 to δ 5.8. These signals correlates to the primary amine and the pyrrole group respectively. In addition, the signal for the methyl group appears as singlet at δ 2.13 (Boechat et al., 2011). It is well-known that the chemical shift of these groups are dependent on hydrogen bonding, temperature and concentration of the sample (Silverstain et al., 1991). Although the NMR of the *mta* compound prepared in this work was not recorded, the infrared spectrum and the microanalysis of it corroborates with the success of the synthetic route. Furthermore, the intermediate compound in step I in Figure 2 is original and has never been

characterised by the NMR technique, to our knowledge. This compound, the amino(hydrazinyl)methaniminium acetate, showed chemical shifts of ^{13}C NMR at δ 179.4, 23.1 and 159.8 correlated to acetate and the aminoguanidinium groups respectively.

The hydrogen NMR of the *Hmta* compound showed broad signals in the region of δ 8.07 (DMSO and $CDCl_3$) relative to the pyrrole group, and at δ 5.95 (DMSO) for the amine group, corroborating with the theoretical calculation of the magnetic shielding tensor. This inversion of chemical shift in comparison with those reported for the *mta* is probably related with the absence of electrons shielding effect upon the 1,2,4-triazole ring. The methyl groups of *Hmta* showed chemical shifts at δ 1.96 in DMSO and 2.14 in $CDCl_3$.

The number of ^{13}C NMR chemical shifts observed in the spectra of the 1,2,4-triazole compounds in this work correlates with the proposed structures shown by Figure 1, as well as to the crystal structure of the *Hmta* in Figure 4. The reported ^{13}C NMR data for the 3-amine-5-methyl-1*H*-1,2,4-triazole (*mta*) showed three chemical shifts at δ 159.9 (**C**-NH_2), 154.9 (**C**-CH_3) and 13.2 (C-**C**H_3) in DMSO (Boechat et al., 2011). The attempt to synthesise this compound with excess of acetic acid, however, led to the formation of *Hmta*, which showed ^{13}C chemical shifts in DMSO at δ 159.2, 155.2 and 13.5, and in $CDCl_3$ at δ 157.3, 153.4 and 12.3, which are in agreement with its crystal structure as well as with its theoretical calculations of NMR. Two carbon chemical shifts were also identified in these solvents at δ 173.0 and 21.8 as well as at δ 177.1 and 21.8 that certainly correlates to the carbonyl and methyl groups of the acetate and acetic acid (Silverstain et al., 1991). The stoichiometry involved in the synthetic route of the *mta* is important considering the side reaction (acid – base) that occurred to form the *Hmta* in the presence of acetic acid in excess. The chemical shift of hydrogen and ^{13}C NMR of the *Hmta* is remarkably similar to that of the *mta* reported in the literature, except by the assignments of the signals to the corresponding chemical group (Boechat et al., 2011). The assignments to the chemical shifts in these compounds corroborate with the theoretical calculation of the magnetic shielding tensor.

The chemical shift of the carbon atoms from the phenyl ring of *pta* appear in the range of δ 139.4 to δ 127.7 and the two carbon atoms of the triazole ring around of δ 171.5 and 160.1 in DMSO, CD_3OD and $CDCl_3$. The two carbon atoms for the triazole ring of *mpta* revealed chemical shifts at δ 172.5 and 159.3 as well as at δ 155.2 for the imine group (C=N), in DMSO. The *mpta* showed three carbon chemical shifts nearby of δ 19.3, related to methyl groups.

Although the *mta* was produced by an equimolar reaction in this work, washings of the product with diethyl ether may not been sufficient to clean up the material from the acetic acid that did not react, remaining a small amount in the sample. This allow speculating that this chemical worked as a catalyst in attempt to purify the *mta* with acetone, producing the *mpta* derivative. Therefore, the NMR chemical shift for the acetic acid in the spectrum of *Hmta* as well as its presence in the crystal lattice of this compound is the evidence that corroborate the acetic acid as a catalyst in the reaction between *mta* and acetone.

2.3. Crystallography

The crystallographic data of *Hmta* are shown in Table 1, and its crystal structure by Figure 4. The *Hmta* crystallizes in the monoclinic space group $P2_1/n$ and shows within the unit cell a molecule of acetic acid and an acetate anion for each ionic 1,2,4-triazole ring. The crystal packing is stabilized by two very weak hydrogen bonds of C3-H⋯O1 (2.809 Å) and N3-H⋯O4 (1.748 Å) involving both the molecule of acetic acid and the acetate ion, which is coplanar with the ionic ring of the *Hmta*. The acetic acid molecule describes a parallel plane to the *Hmta* ring. The lengths and bond angles of the *Hmta* are shown in Table 2.

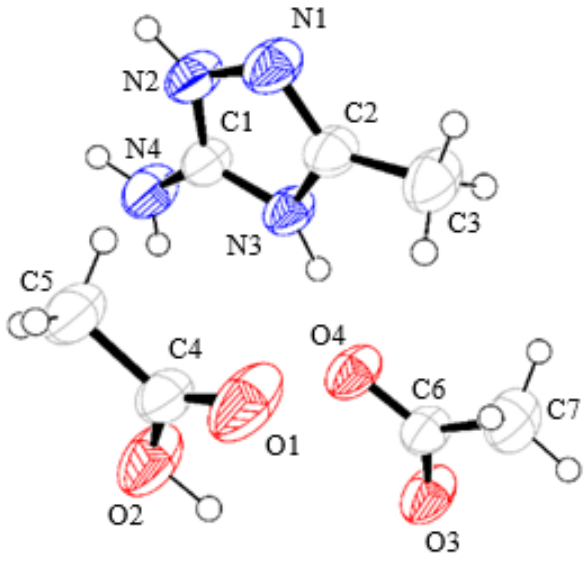

Figure 4 - The Crystal structure of the 3-methyl-1*H*-1,2,4λ^4-triazole-5-amine acetate (*Hmta*).

Table 1 - Crystallographic data for the *Hmta* compound.

Compound	*Hmta*
Chemical Formula	$C_7H_{14}N_4O_4$
Formula weight / g.mol^{-1}	218.22
Crystal system	Monoclinic
Space group	$P2_1/n$
a / Å	7.6420(4)
b / Å	12.0280(5)
c / Å	11.8650(7)
α / °	90
β / °	95.797(6)
γ / °	90
Volume / Å^3	1085.03(9)
Z	4
Temperature / K	293.0(2)
$d_{calc.}$ / g.cm^{-3}	1.336
μ (KαCu) / mm^{-1}	0.110
Radiation	λ = 0.71073 Å (KαMo)
θ limits / °	3.331 - 29.750
Reflections collected / independent	23526 / 2903
Reflections observed [F_{obs}>4$\sigma_{(Fobs)}$]	1920
Parameters	180
R_{int}	0.0575
R indices for [F_{obs}>4$\sigma_{(Fobs)}$]	0.0577
R indices for all data	0.0901
wR indices for [F_{obs}>4$\sigma_{(Fobs)}$]	0.1611
Goodness-of-fit (GOF)	1.001

Table 2 - Selected bond lengths and bond angles of the *Hmta* compound.

Bond lengths / Å			
C1-N2	1.324(2)	C4-O2	1.290(2)
C1-N4	1.330(3)	C4-C5	1.493(3)
C1-N3	1.338(2)	C6-O3	1.246(2)
C2-N1	1.298(2)	C6-O4	1.261(2)
C2-N3	1.375(2)	C6-C7	1.493(3)
C2-C3	1.476(3)	N1-N2	1.384(2)
C4-O1	1.198(2)		
Bond angles / °			
N2-C1-N4	126.6(2)	O2-C4-C5	114.3(2)
N2-C1-N3	106.5(2)	O3-C6-O4	120.8(2)
N4-C1-N3	126.9(2)	O3-C6-C7	119.6(2)
N1-C2-N3	110.8(2)	O4-C6-C7	119.7(2)
N1-C2-C3	125.6(2)	C2-N1-N2	104.4(2)
N3-C2-C3	123.6(2)	C1-N2-N1	111.1(2)
O1-C4-O2	122.8(2)	C1-N3-C2	107.2(1)
O1-C4-C5	122.8(2)		

2.4. Theoretical NMR Approach

Theoretical studies were carried out using software package GAUSSIAN09 (Frisch et al., 2009). Spatial arrangements were used as initial models in geometry optimization calculations. To the *mpta* compound, the tautomeric structures were optimized at post-HF MP4 level (sdq)/6-31G(d,p) resulting in geometry data with good quality and in level DFT/B3LYP/6-311++G(2d,2p), considering solvation by DMSO through the implicit model as shown by Figure 5. This method offers good geometry data with reduced computational cost. The optimized geometries were characterized as true minima on the potential energy surface (PES) when all harmonic frequencies were real. The optimized geometries by MP4 (sdq)/6-31G(d,p), and DFT/B3LYP/6-311++G(2d,2p) were used in carbon chemical shift calculations. The levels of theory B3LYP/6-31G(d,p), B3LYP/6-311+G(d,p), and PBE1PBE/6-311++G(d,p) were applied considering solvation by the DMSO (Jin et al., 2014; Phalgune et al., 2013; Thomas et al., 2005; Ünlüer et al., 2019). The calculated carbon chemical shifts (σ_C) were obtained relative to the corresponding calculated values for tetramethylsilane at the same levels of theory. To define the most adequate level of theory for this work, the correlations between σ_C values and experimental carbon chemical shifts (δ_C) were obtained using software package LibreOffice™ 7.1; σ_C and δ_C values were plotted on the x and y axes, respectively. Correlation curves were given as linear fits with correlation coefficients (R^2) and standard deviations (SD) furnished by the program.

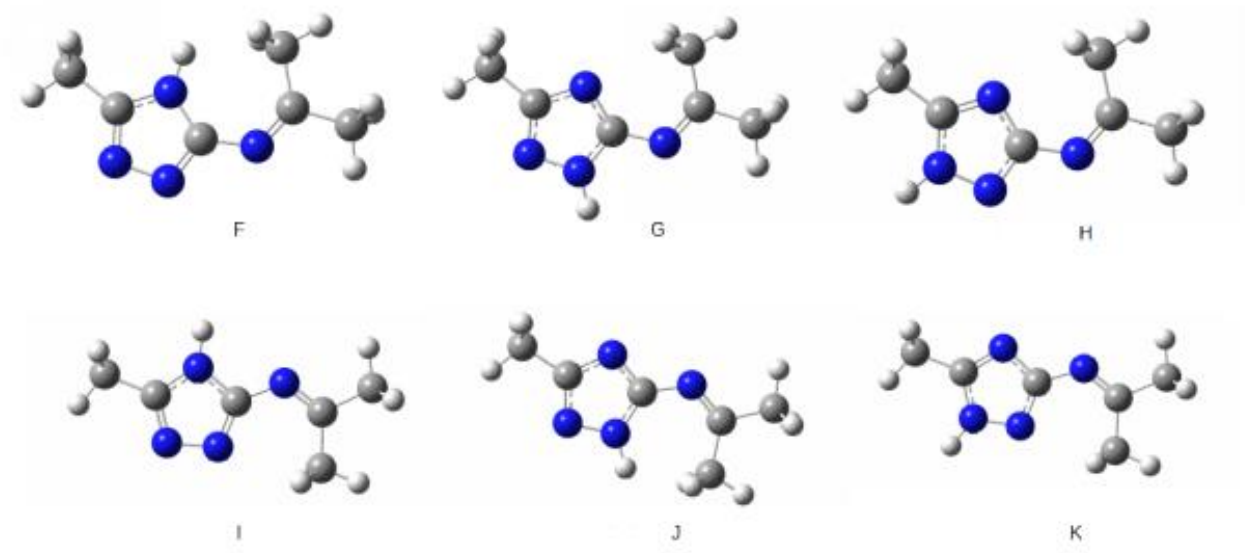

Figure 5 - Optimized structures of *N-(3-methyl-1H-1,2,4-triazole-5-yl)propan-2-imine* (*mpta*) in level B3LYP/6-311++G(2d,2p)/DMSO.

The sets of geometries obtained at levels MP4(sdq)/6-31G(d,p) and B3LYP/6-311++G(2d,2p)/DMSO were submitted to calculus of ^{1}H and ^{13}C NMR at different methods and basis sets as shown in Table 3 that also presents the obtained correlations between σ_C and δ_C. The experimental and calculated NMR data for the *mpta* compound are shown in Tables 4S and 5S (see Supplementary Material).

Table 3 - Correlations between σ_C and δ_C for F, G, H, I, J and K tautomers of *mpta*.

Level of theory	F	G	H	I	J	K
MP4 (SDQ)						
B3LYP/6-31G(d,p)	0.9974	0.9982	0.9956	0.9953	0.9981	0.9960
B3LYP/6-311+G(d,p)	0.9968	0.9979	0.9953	0.9949	0.9978	0.9957
PBE1PBE/6-311++G(d,p)	0.9969	0.9978	0.9954	0.9947	0.9979	0.9958
DFT_DMSO						
B3LYP/6-31G(d,p)	0.9953	0.9982	0.9972	0.9960	0.9979	0.9972
B3LYP/6-311+G(d,p)	0.9946	0.9975	0.9967	0.9954	0.9974	0.9967
PBE1PBE/6-311++G(d,p)	0.9945	0.9973	0.9967	0.9951	0.9972	0.9966

The calculated hydrogen NMR data for the NH group revealed an active hydrogen atom due to the lower calculated chemical shift in comparison with the experimental data (Jin et al., 2014; Phalgune et al., 2013). In general, the computational data with good correlation (0.9934 – 0.9982) were similar to the calculations in gaseous phase (MP4) and DFT, considering solvation by DMSO through the implicit model. At the calculation levels used, the best association shows that the G structure corresponds to the most stable isomer, with a percentage error of 0.41%, suggesting that this molecule may coexist in solution and in the solid state. Among the other molecules shown by Figure 5, structure F corresponds to the less stable tautomer with $\Delta E_{G\text{-}F}$/Kcal·mol^{-1} = 13.63 and 14.27 for optimizations in DFT/DMSO and MP4(SDQ) respectively. This data allow to speculate that tautomeric species such as the structures G, H, I, J and K can be formed in solution, during the reaction path, as the result of a forbidden rotation by resonance effect in the bonding between the 1,2,4-triazole ring and the –C=N$(CH_3)_2$ group.

The optimum theoretical association for the chemical shift calculus of ^{1}H and ^{13}C NMR at different density functional theory methods for the *mta*, *Hmta* and *pta* compounds was obtained using the optimized geometry in level B3LYP/6-311++G(2d,2p) in DMSO or $CDCl_3$ as solvent. The calculated and experimental NMR chemical shifts for the *Hmta* and *mta* compounds are shown in Table 6S and 7S (see Supplementary Material) and Figure 6 shows the optimized structures for these compounds. The experimental NMR data of *mta*, reported in the literature, was the source for comparison with the theoretical calculation. In general, the correlation coefficient between the calculated chemical shifts and the experimental data was satisfactory to all level of theory applied for these triazole compounds. Higher correlation and less error was found using the theoretical levels of B3LYP/6-311+G(d,p) and PBE1PBE/6-311++G(d,p) for the *mta* with the correlations around 0.9996. The resulting calculation has indicated that the tautomer *mta*-A' is the most probable structure in solution. For the *Hmta*, the B3LYP/6-311++G(2d,2p) level of theory provided the best calculated data in comparison to its experimental NMR chemical shifts; the optimized structure for this compound was based on its crystal structure shown by Figure 4.

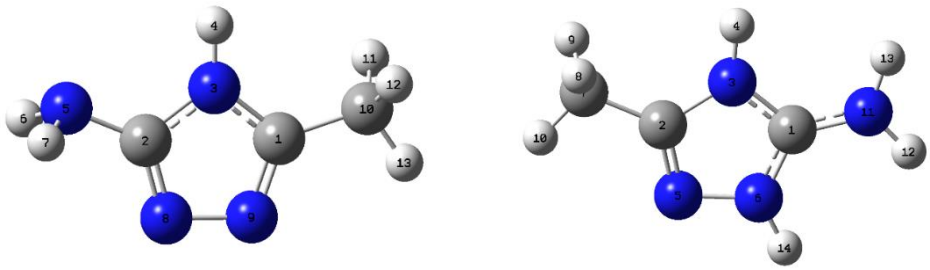

Figure 6 - Optimized structure of 3-methyl-1*H*-1,2,4-triazole-5-amine (*mta*, left) and 3-methyl-1*H*-1,2,4λ^{4}-triazole-5-amine acetate (*Hmta*, right).

Nevertheless, the calculated and experimental ^{13}C chemical shifts of *Hmta* and *mta*, shown in Table 6S and 7S (see Supplementary Material), are remarkably similar with the exception of the exchanging in chemical shift associated to the carbon atoms of these compounds. This exchanging result appears be correlated to the deshielding effect of the positive charge in the ring of *Hmta*, contrasting with the shielding effect in the *mta*. As shown in Table 7S, the chemical shift calculation for the NH hydrogen of the *mta*-A' was at δ 2.5949 by the B3LYP/6-311+G(d,p) and at δ 2.5227 by the PBE1PBE/6-311++G(d,p) levels of theory. These shifts are lower compared to those reported in the literature (δ 6.3-5.8), suggesting that this hydrogen atom is active by hydrogen bonding or tautomerism (Jin et al., 2014; Phalgune et al., 2013). The percentage error in the calculated chemical shift of the carbon atom from the group **C**(NH_2), compared with the reported experimental data, was 0.41% and 1.14% by the levels of theory B3LYP/6-311+G(d,p) and PBE1PBE/6-311++G(d,p). The calculation by these levels of theory shows good correlation with the experimental data, which are 0.99967 and 0.99966, respectively. The difference between the calculated chemical shifts and the experimental data for the *Hmta* in Table 6S is probably due to the solvent effect. Regardless of that, the experimental data in $CDCl_3$ show better accuracy in the correlation between theoretical and experimental data for the ^{1}H and ^{13}C NMR.

The data in Table 8S (see Supplementary Material) shows the calculated NMR chemical shifts for isomeric structures of *pta*. The theoretical approach by the B3LYP/6-311+G(d,p) and PBE1PBE/6-311++G(d,p) bases set reveals that the isomers B and C shown by Figure 3 are good candidates to be considered as stable structures. The energy difference between these structures (ΔE_{B-C}) is 0,2 Kcal·mol^{-1} which reinforces the possibility of tautomerism in solution. It is conceivable, therefore, that both tautomers coexist in solution. However, considering the chemical shift of the group **C**(NH_2), the percentage error for the B3LYP/6-311+G(d,p) base set was 1.00 % (B) and 0.93% (C), and for the PBE1PBE/6-311++G(d,p) 2.03% (B) and 0.39% (C). They all show good correlation with the experimental values which are 0.99849 (B) and 0.99839 (C) for B3LYP/6-311+G(d,p), and 0.99801 (B) and 0.99830 (C) for PBE1PBE/6-311++G(d,p). The less percentage

error for the isomer C by both level of theory suggest this isomer is the most probable in solution as shown by Figure 7. Yet again, the calculated chemical shift for the hydrogen of the NH group is also below that of the experimental data, suggesting an active hydrogen atom by hydrogen bonding or tautomerism (Jin et al., 2014; Phalgune et al., 2013).

The proposed isomeric structures D and E shown by Figure 3 probably does not exist in solution, considering that the chemical shift calculated is far from the experimental data to all bases set in the calculation. In addition to that, they show a great difference in energy in comparison to the isomer C (ΔE_{D-C} and ΔE_{E-C}) which are 20.2 and 11.9 Kcal·mol^{-1} respectively.

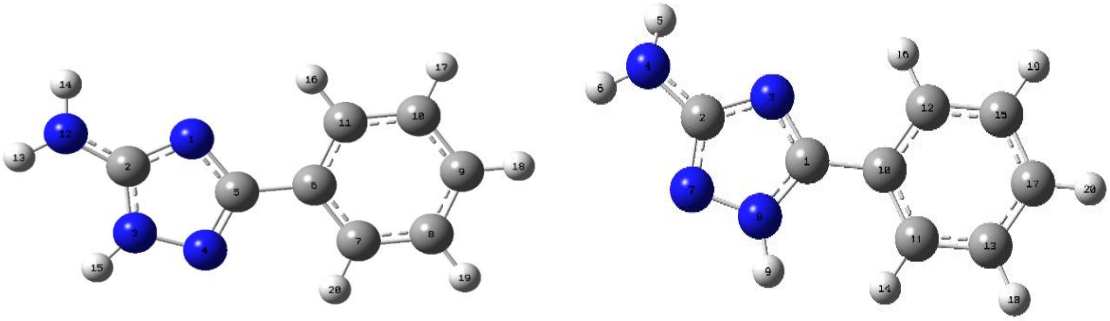

Figure 7 - Optimized structures of isomers B (left) and C (right) of 3-phenyl-1H-1,2,4-triazole-5-amine (*pta*).

2.5. Antimicrobial Activity

The 1,2,4-triazole compounds showed to be inactive against microorganisms Gram-positives (*Staphylococcus aureus* - ATCC 33591; *Bacillus subtilis* - ATCC 23858) and Gram-negatives (*Escherichia coli* - ATCC 29214; *Salmonella typhimurium* - ATCC 14028). The literature reports antimicrobial activity on 1,2,4-triazole compounds having bulky substituent groups bonded to the ring (El Akri et al., 2007; Karthikeyan et al., 2008). The absence of this chemical feature in the compounds tested allow speculating that their inactivity is correlated to this chemical property.

3. Materials and methods

All chemicals purchased from Sigma-Aldrich were used without prior purification. Elemental analysis data were collected from a Perkin Elmer 200 CHNS Elemental Analyzer. The infrared spectra were recorded on a Perkin Elmer FT-IR 1000 using Nujol between CsI windows, and NMR spectra on a Varian 300 MHz as well as in a Bruker Avance DRX-400 MHz apparatus. The TMS was the internal standard reference. The theoretical approach calculation concerning the NMR chemical shifts of the triazole compounds were performed by the GAUSSIAN09 package (Frisch et al., 2009).

3.1. Synthesis of The Triazole Compounds

<u>3-Methyl-1H-1,2,4-triazole-5-amine (*mta*):</u> The synthesis of this compound followed the route described in the literature with slight modifications (Boechat et al., 2011). Into a bottom flask of 250 mL, an equimolar mixture of aminoguanidine bicarbonate and acetic acid (1.5 % excess) were stirred until complete release of carbon dioxide as by-product. After that, 120 mL of toluene was added to the mixture, and the flask fixed to a Dean-stark. The mixture was heated at 120 °C, stirring under reflux, during 22 h. Then, the white material that precipitated at the bottom of the flask was filtered off under reduced pressure. Afterwards, washed with diethyl ether and kept on desiccators. A few crystals of 3-methyl-1*H*-1,2,4λ^4-triazole-5-amine acetate (*Hmta*) were separated after cooling the filtrate.

Yield of 2.5 g (85 %); Mp (°C): 130.8 - 133.1. Elemental analyses required for $C_3H_6N_4$: C, 36.73; H, 6.16; N, 57.11; Found: C, 38.10; H, 6.41; N, 56.71. IR (Nujol / CsI): 3314, 3449 ν(N-H), 3186 $\nu_{as}(NH_2)$; 3039$\nu_s(NH_2)$; 1629, 1666 ν(C=N); 2881 $\nu(CH_3)$.

3-Methyl-1H-1,2,4λ^4-triazole-5-amine acetate *(Hmta)*: The synthesis of this compound followed the technique used in the preparation of *mta* with the exception that a great excess of acetic acid (5.0 mL, 60%, 87.27 mmol) was added to the aminoguanidine bicarbonate (5.16 g, 37.91 mmol). A white material also precipitated and was filtered off under reduced pressure, washed with diethyl ether, and kept on desiccators. Suitable crystals of 3-methyl-1*H*-1,2,4λ^4-triazole-5-amine acetate (*Hmta*) for X-ray analysis were obtained from the filtrate after three days at low temperature.
^{1}H NMR (DMSO, 400 MHz, δ): 8.07 (broad, NH_2); 5.95(broad, NH); 1.96 (s, CH_3). ^{13}C NMR (DMSO, 100 MHz, δ): 159.27 (C-NH_2); 155.28 (C-CH_3); 13.5 (CH_3); 173.0 (R**C**OO^-); 21.8 (**C**H_3COO^-). ^{1}H NMR ($CDCl_3$, 400 MHz, δ): 9.24 (broad, NH_2); 2.14 (s, CH_3). ^{13}C NMR ($CDCl_3$, 100 MHz, δ): 157.3 (C-NH_2); 153.4 (C-CH_3); 12.3 (CH_3); 177.1 (R**C**OO^-); 21.8 (**C**H_3COO^-)

3-Phenyl-1H-1,2,4-triazole-5-amine (*pta*): This compound was synthesised by the same equimolar reaction route described for the *mta* using the benzoic acid as reactant, dissolving it in 7.0 mL of hot water. After releasing the carbon dioxide completely, A Dean-stark was fixed to the flask and the mixture maintained in stirring under reflux. The white material was removed by filtration under reduced pressure followed by washings with diethyl ether and kept on desiccators. No crystals were isolated from the filtrate after cooling at low temperature for three days. Yield of 1.8 g (63 %); Mp (°C): 179.8 - 181.5. Elemental analyses required for $C_8H_8N_4{\cdot}{}^3/_2H_2O$: C, 51.33; H, 5.92; N, 29.93; Found: C, 50.19; H, 6.53; N, 30.13. IR (Nujol / CsI): 3407 $\nu(H_2O)$, 3361 $\nu_{as}(NH_2)$; 3274 $\nu_s(NH_2)$; 1682, 1668 ν(C=N); 841 δ(C-H); 711 δ(C-H). ^{1}H NMR (DMSO-d_6, 300 MHz, δ): 8.13 (NH_2), 10.31 (s, NH), 7.31 (m, Ph, 3H, ^1J (H-H) = 7.01 Hz), 7.88 (m, Ph, 2H, ^1J (H-H) = 7.42 Hz). ^{13}C NMR (DMSO-d_6, 75 MHz, δ): 171.5 (C-NH_2), 160.1 (C-Ph), 139.4, 129.7, 129.3, 127.7 (Ph). ^{1}H NMR (CD_3OD, 300 MHz, δ): 8.13 (NH_2), 10.32 (s, NH), 7.43 (m, Ph, 3H, ^1J (H-H) = 7.01 Hz), 7.93 (m, Ph, 2H, ^1J (H-H) = 7.42 Hz). ^{13}C NMR (CD_3OD, 75 MHz, δ): 174.5 (C-NH_2), 159.8 (C-Ph), 137.6, 130.2, 129.0, 127.6 (Ph). ^{1}H NMR ($CDCl_3$, 300 MHz, δ): 8.24 (NH_2), 10.45 (s, NH), 7.32 (m, Ph, 3H, ^1J (H-H) = 7.01 Hz), 7.89 (m, Ph, 2H, ^1J (H-H) = 7.42 Hz). ^{13}C NMR ($CDCl_3$ 75 MHz, δ): 171.7 (C-NH_2), 160.4 (C-Ph), 139.7, 130.0, 129.6, 128.0 (Ph).

N-(3-Methyl-1H-1,2,4-triazole-5-yl)propan-2-imine (*mpta*): The attempt of purifying the *mta* led to the synthesis of the *mpta* by dissolving 1.00 g of *mta* in acetone (50 mL) at the room temperature. A light yellowish solid was obtained almost immediately. The mixture was kept under stirring for 30 minutes and the solid filtered off in air followed by washings with diethyl ether and stored on desiccators. Mp (°C): 154.9 - 156.3. Elemental analyses required for $C_6H_{10}N_4{\cdot}2H_2O$: C, 41.37; H, 8.10; N, 32.16; Found: C, 40.82; H, 7.81; N, 32.58. IR (Nujol / CsI): 3360 ν(N-H, H_2O); 1692, 1614, 1579 ν(C=N); 780 δ(C-H); 709 δ(C-H). ^{1}H NMR (DMSO-d_6, 300 MHz, δ): 11.06 (broad, NH), 2.17 (s, CH_3), 2.04 (s, CH_3), 1.88 (s, CH_3). ^{13}C NMR (DMSO, 75 MHz, δ): 172.5 (C-NH_2), 159.3 (C-CH_3), 155.2 (C=N), 23.2 (CH_3), 21.4 (CH_3), 13.4 (CH_3).

3.2. Minimum Inhibitory Concentration (MIC)

The broth microdilution assays, using microplates of 96 wells, was the method used to determine the minimum inhibitory concentration (Zacchino & Gupta, 2007). The standard solution of the triazole compounds is composed by 1.0 mg of the substance to be biologically assayed, 250 µL of DMSO and 750 µL of sterile water. The microorganisms were grown in 3.0 mL of the Luria Bertani (LB) broth at 37 °C until reaching an optical density (OD) between 0.08 and 0.10 that corresponds to a range from 1.0 to 2.0 x 10^8 colony-forming unit (CFU) / mL. The LB medium {100 µL (5.0 x 10^4 CFU)} was added to 50 µL of the standard solution of the substance to be tested from each of the bacteria broths. Subsequently, the mixture was poured into the wells of the plates and

incubated for 24 h. The MIC was analysed using a spectrometer ELISA at 600 nm. The experiment was carried out in duplicate, considering the standard deviation. *Amoxicillin* and *Norfloxacin* were used as positive control and DMSO as negative control.

3.3. Single Crystal X-ray Diffraction

Crystallographic data were collected using a Bruker Kappa CCD diffractometer with MoKα (λ = 0.71073 Å) at room temperature. Data collection, reduction and refinement of the unit cell array were performed by the programs COLLECT (Nonius, Delft) , EVALCCD (Duisenberg, 1992) and DIRAX (Duisenberg, Kroon-Batenburg, & Schreurs, 2003). The structure was solved and refined using SHELXL-97 (Sheldrick, 1997). The absorption correction was applied to all atoms and assigned to the anisotropic displacement parameters except for the hydrogen atom (Blessing, 1995). The displacement parameters of H atoms were fixed at 1.2 U_{eq} of the carbon atoms. The maximum peak and deepest hole observed in the final Δρ map were 0.158 and -0.165 e.$Å^{-3}$. The structures were drawn by ORTEP-3 for Windows (Farrugia, 1997) and Mercury (Macrae et al., 2006) programs.

Crystallographic Data: X-ray crystallographic data for the 3-methyl-1*H*-1,2,4λ^4-triazole-5-amine acetate (*Hmta*) has been deposited with the Cambridge Crystallographic Data Centre, 12 Union Road, Cambridge CB2 1EZ, UK; Fax: +44(0)1233 336033, e-mail: deposit@ccdc.cam.ac.uk. It can be obtained free of charge by request at www.ccdc.cam.ac.uk/conts/retrieving.html, quote CCDC 1832920.

3.4. Theoretical NMR Data

The structure of the compounds were drawn in GaussView. Subsequently were submitted to geometrical optimization by means of the MP4 and DFT methods by the GAUSSIAN09 software. Chemical shifts were obtained by the shielding tensor values of NMR which were calculated for the optimized structure at B3LYP/6-31G(d,p), B3LYP/6-311+G(d,p), PBE1PBE/6-311++G(d,p), and B3LYP/6-311++G(2d,2p) levels of theory. The TMS was the shielding tensor reference for for the calculated chemical shifts.

4. Conclusion

Simple molecules of triazole compounds have been synthesised and had their biological activity tested. These compounds did not show biological activity against strains of Gram-positive and Gram-negative microorganisms at the highest concentration tested. The novel compounds *Hmta*, *pta* and *mpta* were synthesised by the methodology described in the literature, although the reaction pathway seems to be dependent on the amount of reactants as reveal by the synthesis of *Hmta*.

The computational approach shows that the high values of the correlation coefficient between the theoretical and experimental data obtained for these triazole compounds was influenced by the insertion of diffuse functions. In this context, it is conceivable that the presence of additional parameters to the calculation such as inter and intramolecular hydrogen bonding might provide better accuracy in the resulting theoretical data. Nevertheless, the calculated NMR data corroborate with the acid-base reaction of the *Hmta*, supported by its crystal structure. Beyond that, the theoretical data suggest not only the tautomerism but also the most probable tautomers in solution for the *mta*, *pta* and the *mpta* compounds.

5. Supplementary Material

Tables containing the NMR chemical shift and the shielding tensor calculations are free access at the JCEC website as Supplementary Material for the triazole compounds prepared in this work.

Acknowledgements

The authors appreciate the financial support of the Coordenação de Aperfeiçoamento de Pessoal de Nível Superior - Brasil (CAPES) - Finance Code 001 as well as to the Brazilian agencies FAPEMIG and CNPq.

References

Abdel-Megeed, A. M., Abdel-Rahman, H. M., Alkaramany, G.-E. S., & El-Gendy, M. A. (2009). Design, synthesis and molecular modeling study of acylated 1,2,4-triazole-3-acetates with potential anti-inflammatory activity. *European Journal of Medicinal Chemistry, 44*(1), 117-123. doi:http://dx.doi.org/10.1016/j.ejmech.2008.03.017

Akerblom, E., & Sandberg, M. (1965). Alkyl Derivatives of 3-amino-5-(2-furyl)-1,2,4-triazole. *Acta Chimica Scandinavica, 19*, 1191-1204. doi:10.3891/acta.chem.scand.19-1191

Blessing, R. H. (1995). An empirical correction for absorption anisotropy. *Acta Crystallographica, Section A: Foundations of Crystallography, 51*, 33-38. doi:10.1107/S0108767394005726

Boechat, N., Pinheiro, L. C. S., Santos-Filho, O. A., & Silva, I. C. (2011). Design and Synthesis of New N-(5-Trifluoromethyl)-1H-1,2,4-triazol-3-yl Benzenesulfonamides as Possible Antimalarial Prototypes. *Molecules, 16*(9), 8083. doi:https://doi.org/10.3390/molecules16098083

Deng, X.-Q., Song, M.-X., Zheng, Y., & Quan, Z.-S. (2014). Design, synthesis and evaluation of the antidepressant and anticonvulsant activities of triazole-containing quinolinones. *European Journal of Medicinal Chemistry, 73*, 217-224. doi:http://dx.doi.org/10.1016/j.ejmech.2013.12.014

Duisenberg, A. J. M. (1992). Indexing in single-crystal diffractometry with an obstinate list of reflections. *Journal of Applied Crystallography, 25*, 92-96. doi: https://doi.org/10.1107/S0021889891010634

Duisenberg, A. J. M., Kroon-Batenburg, L. M. J., & Schreurs, A. M. M. (2003). An intensity evaluation method: EVAL-14. *Journal of Applied Crystallography, 36*, 220-229. https://doi.org/10.1107/S0021889802022628

El Akri, K., Bougrin, K., Balzarini, J., Faraj, A., & Benhida, R. (2007). Efficient synthesis and in vitro cytostatic activity of 4-substituted triazolyl-nucleosides. *Bioorganic & Medicinal Chemistry Letters, 17*(23), 6656-6659. doi:http://dx.doi.org/10.1016/j.bmcl.2007.08.077

Farrugia, L. J. (1997). ORTEP-3 for windows - a version of ORTEP-III with a graphical user interface (GUI). *Journal of Applied Crystallography, 30*(5), 565-565. doi:10.1107/S0021889897003117

Frisch, M. J., G.W. Trucks, Schlegel, H. B., Scuseria, G. E., Robb, M. A., Cheeseman, J. R., . . . Fox., D. J. (2009). Gaussian 09, Revision E.01, Gaussian, Inc., Wallingford CT.

Graci, J. D., & Cameron, C. E. (2006). Mechanisms of action of ribavirin against distinct viruses. *Reviews in Medical Virology, 16*(1), 37-48. doi:10.1002/rmv.483

Grinshtein, V. Y., Strazdin, A. A., & Grinvalde, A. K. (1970). Infrared absorption spectra of some C-halogenated 1, 2, 4-triazole derivatives. *Chemistry of Heterocyclic Compounds, 6*(2), 231-239. doi:10.1007/bf00475004

Groll, A. H., Piscitelli, S. C., & Walsh, T. J. (1998). Clinical Pharmacology of Systemic Antifungal Agents: A Comprehensive Review of Agents in Clinical Use, Current Investigational Compounds, and Putative Targets for Antifungal Drug Development. In M. W. A. F. M. J. Thomas August & T. C. Joseph (Eds.), *Advances in Pharmacology* (Vol. Volume 44, pp. 343-500): Academic Press.

Han, L. P., Wang, X., Guo, X., Rao, M. S., Steinberger, Y., Cheng, X., & Xie, G. H. (2011). Effect of plant growth regulators on growth, yield and lodging of sweet sorghum. *Research on Crops, 12*(2), 372-382. https://www.researchgate.net/publication/279890538

Jin, R. Y., Sun, X. H., Liu, Y. F., Long, W., Lu, W. T., & Ma, H. X. (2014). Synthesis, crystal structure, IR, 1H NMR and theoretical calculations of 1,2,4-triazole Schiff base. *Journal of Molecular Structure, 1062*, 13-20. doi:https://doi.org/10.1016/j.molstruc.2014.01.010

Johnson, E. M., Szekely, A., & Warnock, D. W. (1999). In Vitro Activity of Syn-2869, a Novel Triazole Agent, against Emerging and Less Common Mold Pathogens. *Antimicrobial Agents and Chemotherapy, 43*(5), 1260-1263. https://doi.org/10.1128/AAC.43.5.1260

Karthikeyan, M. S., Holla, B. S., & Kumari, N. S. (2008). Synthesis and antimicrobial studies of novel dichlorofluorophenyl containing aminotriazolothiadiazines. *European Journal of Medicinal Chemistry, 43*(2), 309-314. doi:http://dx.doi.org/10.1016/j.ejmech.2007.03.024

Lopyrev, V. A., Beresneva, N. K., & Strelets, B. K. (1969). Infrared spectra and structure of some 3,5-diamino-1,2, 4-triazoles (guanazoles). *Chemistry of Heterocyclic Compounds, 5*(4), 544-546. doi:10.1007/bf00470284

Macrae, C. F., Edgington, P. R., McCabe, P., Pidcock, E., Shields, G. P., Taylor, R., . . . van De Streek, J. (2006). Mercury: visualization and analysis of crystal structures. *Journal of Applied Crystallography, 39*, 453-457. doi:10.1107/s002188980600731x

Naito, Y., Akahoshi, F., Takeda, S., Okada, T., Kajii, M., Nishimura, H., . . . Kagitani, Y. (1996). Synthesis and Pharmacological Activity of Triazole Derivatives Inhibiting Eosinophilia. *Journal of Medicinal Chemistry, 39*(15), 3019-3029. doi:10.1021/jm9507993

Nonius, B. V. (Delft). COLLECT (1997-2000) Enraf-Nonius. The Netherlands.

Papakonstantinou-Garoufalias, S., Pouli, N., Marakos, P., & Chytyroglou-Ladas, A. (2002). Synthesis antimicrobial and antifungal activity of some new 3-substituted derivatives of 4-(2,4-dichlorophenyl)-5-adamantyl-1H-1,2,4-triazole. *Il Farmaco, 57*(12), 973-977. doi:http://dx.doi.org/10.1016/S0014-827X(02)01227-2

Phalgune, U. D., Vanka, K., & Rajamohanan, P. R. (2013). GIAO/DFT studies on 1,2,4-triazole-5-thiones and their propargyl derivatives. *Magnetic Resonance in Chemistry, 51*(12), 767-774. doi:https://doi.org/10.1002/mrc.4012

Roberts, J., Schock, K., Marino, S., & Andriole, V. T. (2000). Efficacies of Two New Antifungal Agents, the Triazole Ravuconazole and the Echinocandin LY-303366, in an Experimental Model of Invasive Aspergillosis. *Antimicrobial Agents and Chemotherapy, 44*(12), 3381-3388. doi:10.1128/aac.44.12.3381-3388.2000

Sheldrick, G. M. (1997). SHELXL-97 - A Program for Crystal Structure Refinement: University of Goettingen, Germany.

Silverstain, R. M., Bassler, G. C., & Morril, T. C. (1991). *Spectrometric Identification of Organic Compounds* (Fifth ed.). New York: John Wiley & Sons, INC.

Sokmen, B. B., Gumrukcuoglu, N., Ugras, S., Sahin, H., Sagkal, Y., & Ugras, H. I. (2015). Synthesis, Antibacterial, Antiurease, and Antioxidant Activities of Some New 1,2,4-Triazole Schiff Base and Amine Derivatives. *Applied Biochemistry and Biotechnology, 175*(2), 705-714. doi:10.1007/s12010-014-1307-2

Sudheendran, K., Schmidt, D., Frey, W., Conrad, J., & Beifuss, U. (2014). Facile synthesis of 3,5-diaryl-1,2,4-triazoles via copper-catalyzed domino nucleophilic substitution/oxidative cyclization using amidines or imidates as substrates. *Tetrahedron, 70*(8), 1635-1645. doi:http://dx.doi.org/10.1016/j.tet.2014.01.019

Thomas, S., Biswas, N., Venkateswaran, S., Kapoor, S., D'Cunha, R., & Mukherjee, T. (2005). Raman, infrared, SERS and DFT calculations of a triazole derivative (akacid). *Chemical Physics Letters, 402*(4), 361-366. doi:https://doi.org/10.1016/j.cplett.2004.12.064

Tyagi, P., Tyagi, M., Agrawal, S., Chandra, S., Ojha, H., & Pathak, M. (2017). Synthesis, characterization of 1,2,4-triazole Schiff base derived 3d-metal complexes: Induces cytotoxicity in HepG2, MCF-7 cell line, BSA binding fluorescence and DFT study. *Spectrochimica Acta Part A: Molecular and Biomolecular Spectroscopy, 171*, 246-257. doi:http://dx.doi.org/10.1016/j.saa.2016.08.008

Ünlüer, D., Ünver, Y., Düğdü, E., Alpaslan, Y. B., Köysal, Y., Soylu, M. S., & Sancak, K. (2019). Novel 1,2,4-Triazole Derivatives: Structure, DFT Study, X-Ray Analysis, and Antimicrobial

Activity. *Russian Journal of Organic Chemistry, 55*(2), 254-261. doi:10.1134/s1070428019020192

Vatmurge, N. S., Hazra, B. G., Pore, V. S., Shirazi, F., Chavan, P. S., & Deshpande, M. V. (2008). Synthesis and antimicrobial activity of β-lactam–bile acid conjugates linked via triazole. *Bioorganic & Medicinal Chemistry Letters, 18*(6), 2043-2047. doi:http://dx.doi.org/10.1016/j.bmcl.2008.01.102

Vieira, F. T., Maia, J. R. D., Ardisson, J. D., & de Lima, G. M. (2008). Carbonate and Semicarbazide Tin(IV) Derivatives of Aminoguanidine Bicarbonate. *Main Group Metal Chemistry, 31*(1-2), 1-11. https://doi.org/10.1515/MGMC.2008.31.1-2.1

Wajda-Hermanowicz, K., Pieniążczak, D., Wróbel, R., Zatajska, A., Ciunik, Z., & Berski, S. (2016). A study on the condensation reaction of aryl substituted 4-amine-1,2,4-triazole with benzaldehydes: Structures and spectroscopic properties of schiff bases and stable hemiaminals. *Journal of Molecular Structure, 1114*, 108-122. doi:http://dx.doi.org/10.1016/j.molstruc.2016.02.047

Wu, J., Liu, X., Cheng, X., Cao, Y., Wang, D., Li, Z., De Clercq, E. (2007). Synthesis of Novel Derivatives of 4-Amino-3-(2-Furyl)-5-Mercapto-1,2,4-Triazole as Potential HIV-1 NNRTIs. *Molecules*, *12*(8), 2003-2016. doi: 10.3390/12082003

Zacchino, S. A., & Gupta, M. P. (2007). *Manual de técnicas in vitro para la deteccíon de compuestos antifúngicos*: Corpus Libros Médicos y Científicos.

Supplementary Material

1. Calculating chemical shifts using a reference compound

Quantum mechanical calculations of Nuclear Magnetic Resonance (NMR) parameters, such as chemical shifts and coupling constants, have become a very popular tool for structural elucidation of synthetic and natural product in the field of chemistry. The calculations of NMR chemical shifts are extensively used in the validation of chemical structures. To calculate the chemical shifts of a compound, the NMR isotropic shielding tensor (r) is firstly calculated. These calculations uses quantum mechanical methods and the most common are the density functional theory (DFT), and the perturbation theory or higher-level post-Hartree-Flock (HF). The DFT methods have become very popular, as there is a good correlation between accuracy and efficiency with several DFT functions available. The conversion of calculated NMR isotropic shielding tensors of a specific compound into its chemical shift is achieved using tetramethylsilane (TMS) as the reference compound; the same calculating methodology applies for both compounds. The chemical shifts for the novel compound are obtained by subtracting from the isotropic magnetic shielding tensor of this compound, the isotropic magnetic shielding tensor of the reference (TMS). The analysis of the data is performed by linear correlation, plotting the calculated chemical shifts against the experimental data. Considering the fact that, the computational methods are performed in different conditions, in comparison to a real experiment, and that the NMR spectroscopy method is sensitive to short-range structural changes, it is expected systematic differences between the calculated and the experimental chemical shifts. Therefore, it is reasonable to use correlation coefficients to improve the accuracy predicted by DFT, for comparison between the experimental and theoretical data, in ^{13}C NMR chemical shifts. Additionally, the ^{1}H NMR data for the methyl signals are averaged across the chemical shifts of the three stationary hydrogens (References 1S, 2S, 3S, 4S, 5S). The calculated and experimental data of the 1,2,4-triazole compounds are shown in Tables 4S to 8S.

Table 4S. - Experimental and calculated† NMR data for the *mpta* (F, G, H, I, J, K) tautomer, with geometry optimization data obtained in MP4(sdq)/6-31G(d,p).

	δ Exp.	F	G	H	I	J	K
B3LYP/6-31G(d,p)							
C**H**$_3$	1.88	1.9313	2.1938	2.1907	2.1881	2.0285	2.2202
C**H**$_3$	2.04	2.8774	2.2364	2.2402	2.2628	2.2381	2.3551
C**H**$_3$	2.17	2.2998	2.4518	2.3612	2.4849	2.3041	2.2383
N**H**	11.06	8.0165	9.1589	9.2393	8.0004	9.0598	9.1920
C(**C**H$_3$)	13.4	12.6817	16.0721	13.7841	12.4401	15.5872	13.5791
C(**C**H$_3$)	21.4	21.9877	26.1920	25.7869	26.9956	23.5134	26.6178
C(**C**H$_3$)	23.2	31.7884	31.4957	32.17191	31.3402	32.3243	31.9925
C(**C**-N)	155.2	142.6782	153.2574	144.9860	142.3628	153.3554	146.5157
C(**C**-CH$_3$)	159.3	151.3214	157.7380	164.2170	153.6228	158.3381	164.4159
C(N=**C**)	172.5	160.2246	173.9528	169.9458	173.2153	168.4404	170.7136
CTE		0.9974	0.9982	0.9956	0.9953	0.9981	0.9960
B3LYP/6-311+G(d,p)							
C**H**$_3$	1.88	1.9743	2.3202	2.3180	2.3075	2.0975	2.3450
C**H**$_3$	2.04	2.3590	2.3870	2.3428	2.3697	2.3918	2.3450
CH$_3$	2.17	2.3980	2.5409	2.4594	2.5846	2.4044	2.3488
N**H**	11.06	8.0957	9.2842	9.3403	8.1819	9.1376	9.2366
C(**C**H$_3$)	13.4	13.9866	17.6273	14.9795	13.2746	16.7743	14.3281
C(**C**H$_3$)	21.4	22.7027	27.7397	27.0385	28.6892	24.3786	28.0151
C(**C**H$_3$)	23.2	35.3024	35.1138	35.6888	34.6928	35.6772	35.3117
C(**C**-N)	155.2	154.4969	166.9054	157.3954	154.0896	166.7495	158.5246
C(**C**-CH$_3$)	159.3	164.6713	170.8895	178.4505	167.1328	171.1797	178.4507
C(N=**C**)	172.5	172.8143	188.7518	184.0080	188.5445	182.0369	185.4970
CTE		0.9968	0.9979	0.9953	0.9949	0.9978	0.9957
PBE1PBE/6-311++G(d,p)							
C**H**$_3$	1.88	1.9750	2.3084	2.2867	2.2867	2.0796	2.3112
C**H**$_3$	2.04	2.3667	2.3550	2.3240	2.3408	2.3536	2.3296
CH$_3$	2.17	2.3927	2.5219	2.4382	2.5629	2.3907	2.3307
N**H**	11.06	8.1183	9.2729	9.3241	8.2197	9.1279	9.2288
C(**C**H$_3$)	13.4	13.7313	17.2371	14.7431	13.1133	16.4391	14.1809
C(**C**H$_3$)	21.4	22.7378	27.8372	27.1300	28.7900	24.4139	28.1330
C(**C**H$_3$)	23.2	34.9207	34.723	35.2681	34.2767	35.3184	34.8880
C(**C**-N)	155.2	153.1771	165.1681	155.8720	152.8528	164.8752	157.1508
C(**C**-CH$_3$)	159.3	162.9664	168.8616	176.2924	165.3159	169.3563	176.1817
C(N=**C**)	172.5	172.0194	187.8613	182.9877	187.5715	181.2009	184.4899
CTE		0.9969	0.9978	0.9954	0.9947	0.9979	0.9958

† Gas phase; CTE (Correlation between Theoretical and Experimental data);

Table 5S -Experimental and calculated‡ NMR data for the *mpta* (F, G, H, I, J, K) tautomer, with geometry optimization data obtained in DFT/B3LYP/6-311++G(2d,2p)/DMSO.

	δ Exp.	F	G	H	I	J	K
B3LYP/6-31G(d,p)							
C**H**$_3$	1.88	2.3364	2.2201	2.2519	2.3060	2.1938	2.2634
C**H**$_3$	2.04	2.3798	2.2262	2.3552	2.3600	2.2585	2.2802
CH$_3$	2.17	2.4140	2.2424	2.3715	2.3760	2.3848	2.3518
N**H**	11.06	9.7900	9.2679	9.8261	8.5773	9.5288	9.8495
C(**C**H$_3$)	13.4	12.6484	15.4422	13.4174	12.3735	15.2158	13.0586
C(**C**H$_3$)	21.4	25.1425	23.1962	25.5889	26.7582	23.6833	26.5460
C(**C**H$_3$)	23.2	36.2768	29.6595	32.3466	31.7583	32.4007	32.1275
C(**C**-N)	155.2	148.6195	152.3899	148.3891	145.6424	151.9002	148.7217
C(**C**-CH$_3$)	159.3	149.2986	156.2343	162.0108	153.3098	156.6014	161.8371
C(N=**C**)	172.5	170.1617	177.4526	171.7264	174.8131	174.5916	172.8955
CTE		0.9953	0.9982	0.9972	0.9960	0.9979	0.9972
B3LYP/6-311+G(d,p)							
C**H**$_3$	1.88	2.4577	2.3532	2.4091	2.4259	2.2747	2.3907
C**H**$_3$	2.04	2.5089	2.3822	2.4624	2.4659	2.4294	2.4161
CH$_3$	2.17	2.5132	2.4488	2.4741	2.4904	2.4992	2.4734
N**H**	11.06	10.0562	9.3835	9.9100	8.7877	9.6222	9.8899
C(**C**H$_3$)	13.4	14.2767	17.2876	15.0080	13.5960	16.7690	14.2200
C(**C**H$_3$)	21.4	26.3880	25.1647	27.1963	28.6643	25.0853	28.2874
C(**C**H$_3$)	23.2	40.7087	33.5601	36.5072	35.5909	36.3311	36.0581
C(**C**-N)	155.2	162.1734	165.7812	161.6629	158.5847	165.8311	161.5289
C(**C**-CH$_3$)	159.3	162.9255	170.0586	176.7136	167.3300	170.0370	176.1470
C(N=**C**)	172.5	186.3183	194.7317	187.6225	191.5178	190.7120	189.3898
CTE		0.9946	0.9975	0.9967	0.9954	0.9974	0.9967
PBE1PBE/6-311++G(d,p)							
C**H**$_3$	1.88	2.4297	2.3388	2.3947	2.4083	2.2647	2.3733
C**H**$_3$	2.04	2.4911	2.3588	2.4375	2.4449	2.3955	2.4043
CH$_3$	2.17	2.5042	2.4144	2.4538	2.4674	2.4893	2.4469
N**H**	11.06	10.0921	9.4070	9.9057	8.8267	9.6288	9.8983
C(**C**H$_3$)	13.4	14.0502	16.9302	14.7648	13.4471	16.4082	14.0490
C(**C**H$_3$)	21.4	26.4177	25.4802	27.2850	28.7518	25.2209	28.4035
C(**C**H$_3$)	23.2	40.3424	33.2568	36.1088	35.2159	35.9973	35.6604
C(**C**-N)	155.2	160.7368	164.1820	160.1080	157.3174	164.0677	160.1518
C(**C**-CH$_3$)	159.3	161.3816	168.3921	174.6293	165.5923	168.2915	173.9931
C(N=**C**)	172.5	185.4207	193.9106	186.8261	190.7821	190.0600	188.6287
CTE		0.9945	0.9973	0.9967	0.9951	0.9972	0.9966

‡ - in DMSO; CTE (Correlation between Theoretical and Experimental data);

Table 6S - Experimental and calculated NMR data for the *Hmta* in DMSO and $CDCl_3$, with geometry optimization data obtained in DFT/B3LYP/6-311++G(2d,2p)/DMSO.

	δ Exp.[a]	δ Exp.[b]	B3LYP/6-311++G(2d,2p)
C**H**$_3$	1.96	2.14	2.6408
N**H (H14)**	8.07	9.24	8.8419
N**H (H4)**	–	–	7.9606
N**H**$_2$	5.95	–	5.1502
CH$_3$	13.5	12.3	12.4075
C(CH$_3$)	159.27	157.3	157.7567
C(NH$_2$)	155.28	153.4	153.1876
CTE			0.99990[a] /0.99998[b]

CTE (Correlation between Theoretical and Experimental data), a - DMSO, b - $CDCl_3$.

Table 7S - Experimental and calculated NMR data for the *mta* (A', B', C') tautomer in DMSO, with geometry optimization data obtained in DFT/B3LYP/6-311++G(2d,2p)/DMSO.

		B3LYP/6-31G(d,p)			B3LYP/6-311+G(d,p)		
	δ Exp[Ø].	A'	B'	C'	A'	B'	C'
C**H**$_3$	2.13	2.1879	1.8285	2.0131	2.3551	2.1839	2.3218
N**H**	6.3-5.8	2.2184	2.1605	2.1575	2.5949	2.3657	2.4324
N**H**$_2$	8.7-8.0	7.8007	8.7885	9.074	7.9294	8.9479	9.1988
CH$_3$	13.2	12.6	15.7898	13.7204	13.7049	17.2689	14.8638
C(CH$_3$)	154.9	141.8918	146.3257	145.8263	154.3362	159.7183	158.6568
C(NH$_2$)	159.9	146.1909	157.1125	158.9454	159.2434	170.6053	173.1401
CTE		0.99961	0.99837	0.99799	0.99967	0.99858	0.99801
		PBE1PBE/6-311++G(d,p)					
C**H**$_3$	2.13	2.3159	2.117	2.2885			
N**H**	6.3-5.8	2.5227	8.9451	2.3703			
N**H**$_2$	8.7-8.0	7.9552	8.9451	9.1751			
CH$_3$	13.2	13.5561	16.9634	14.7349			
C(CH$_3$)	154.9	153.1399	158.4469	157.1857			
C(NH$_2$)	159.9	158.0749	168.7877	171.3344			
CTE		0.99966	0.99918	0.99806			

CTE (Correlation between Theoretical and Experimental data); Ø - Experimental data of *mta* reported in the literature (1S).

Table 8S - Experimental and calculated NMR data for the *pta* (A, B, C, D, E) tautomer in DMSO, with geometry optimization data obtained in DFT/B3LYP/6-311++G(2d,2p)/DMSO.

	δ Exp.	A	B	C	D	E
B3LYP/6-31G(d,p)						
Ph(**H**)	7.01	3.444	3.5867	3.0749	4.7715	4.361
Ph(**H**)	7.31	7.2652	7.2932	7.3956	5.7141	6.4305
Ph(**H**)	7.88	7.3665	7.3719	7.4824	6.4984	6.6796
N**H**$_2$	8.13	7.4082	7.9556	7.9513	7.5392	7.4588
N**H**	10.31	7.794	8.2926	9.2602	7.8672	7.5875
Ph(**C**)	127.7	118.7756	122.1177	120.638	123.4452	119.6325
Ph(**C**)	129.3	122.0468	122.8734	123.8862	123.9173	123.2828
Ph(**C**)	129.7	123.8485	122.9471	123.9325	124.5229	123.8996
Ph(**C**)	139.4	124.6266	128.4737	123.9652	126.9448	123.9105
C-(Ph)	160.2	141.7851	144.5942	147.4558	159.584	139.5523
C-(NH$_2$)	171.5	143.3112	156.6623	157.9429	163.9462	144.0003
CTE		0.99430	0.99860	0.99827	0.99829	0.99377
B3LYP/6-311+G(d,p)						
Ph(**H**)	7.01	3.8542	3.9866	3.5893	5.3561	4.4444
Ph(**H**)	7.31	7.4178	7.4766	7.5752	6.116	6.9045
Ph(**H**)	7.88	7.5507	7.568	7.6302	6.4708	6.9599
N**H**$_2$	8.13	7.5791	8.1586	8.1769	7.7	7.6134
N**H**	10.31	8.0384	8.5515	9.3157	8.0879	7.8089
Ph(**C**)	127.7	129.5644	133.6122	131.7226	134.9004	130.6741
Ph(**C**)	129.3	134.099	134.5331	135.2125	135.4916	134.2305
Ph(**C**)	129.7	135.5979	135.0229	135.5533	135.8739	135.4559
Ph(**C**)	139.4	136.247	140.1653	135.9626	139.2853	135.9371
C-(Ph)	160.2	153.8445	159.4296	159.9258	175.4565	152.0228
C-(NH$_2$)	171.5	157.3631	169.7787	173.1118	177.3422	159.3037
CTE		0.99429	0.99849	0.99839	0.99808	0.99461
PBE1PBE/6-311++G(d,p)						
Ph(**H**)	7.01	3.8491	3.9872	3.5542	5.3095	4.4204
Ph(**H**)	7.31	7.4888	7.5489	7.6536	6.0789	6.9531
Ph(**H**)	7.88	7.5538	7.647	7.7171	6.4758	6.9915
N**H**$_2$	8.13	7.656	8.1725	8.2487	7.7902	7.7
N**H**	10.31	8.1281	8.6353	9.323	8.1718	7.8808
Ph(**C**)	127.7	129.3042	133.1975	131.407	134.6342	130.2974
Ph(**C**)	129.3	133.8465	134.2682	134.1237	134.6773	133.1529
Ph(**C**)	129.7	134.9889	134.7552	135.2025	135.1766	135.0661
Ph(**C**)	139.4	135.2698	138.7849	135.7788	139.0888	135.7645
C-(Ph)	160.2	152.6525	157.6835	158.5392	173.6897	150.7569
C-(NH$_2$)	171.5	155.9194	168.0038	170.8153	175.9921	157.8276
CTE		0.99370	0.99801	0.99830	0.99834	0.99420

CTE (Correlation between Theoretical and Experimental data)

References

1S Boechat, N., Pinheiro, L. C. S., Santos-Filho, O. A., & Silva, I. C. (2011). Design and Synthesis of New N-(5-Trifluoromethyl)-1H-1,2,4-triazol-3-yl Benzenesulfonamides as Possible Antimalarial Prototypes. *Molecules, 16*(9), 8083. doi: https://doi.org/10.3390/molecules16098083

2S Jin, R. Y., Sun, X. H., Liu, Y. F., Long, W., Lu, W. T., & Ma, H. X. (2014). Synthesis, crystal structure, IR, 1H NMR and theoretical calculations of 1,2,4-triazole Schiff base. *Journal of Molecular Structure, 1062*, 13-20. doi:https://doi.org/10.1016/j.molstruc.2014.01.010

3S Phalgune, U. D., Vanka, K., & Rajamohanan, P. R. (2013). GIAO/DFT studies on 1,2,4-triazole-5-thiones and their propargyl derivatives. *Magnetic Resonance in Chemistry, 51*(12), 767-774. doi:https://doi.org/10.1002/mrc.4012

4S Thomas, S., Biswas, N., Venkateswaran, S., Kapoor, S., D'Cunha, R., & Mukherjee, T. (2005). Raman, infrared, SERS and DFT calculations of a triazole derivative (akacid). *Chemical Physics Letters, 402*(4), 361-366. doi:https://doi.org/10.1016/j.cplett.2004.12.064

5S Ünlüer, D., Ünver, Y., Düğdü, E., Alpaslan, Y. B., Köysal, Y., Soylu, M. S., & Sancak, K. (2019). Novel 1,2,4-Triazole Derivatives: Structure, DFT Study, X-Ray Analysis, and Antimicrobial Activity. *Russian Journal of Organic Chemistry, 55*(2), 254-261. doi:https://doi.org/10.1134/S1070428019020192